How transversal fluctuations affect the friction of a particle on a rough incline

S. Dippel,[1,3] G. G. Batrouni,[1,2] and D. E. Wolf[3]
[1]*Höchstleistungsrechenzentrum, Forschungszentrum Jülich, 52425 Jülich, Germany*
[2]*Institut Non-Linéaire de Nice, Université de Nice-Sophia Antipolis, 1361 route des Lucioles, 06560 Valbonne, France*
[3]*Gerhard-Mercator-Universität, FB 10, 47048 Duisburg, Germany*
(Received 25 April 1997)

We present molecular-dynamics simulations of a sphere moving down an inclined plane consisting of similar spheres of smaller size. For a certain range of inclinations, the sphere moves down the plane with a mean velocity $\overline{v_x} \neq 0$. We investigate the properties of the motion in this steady state and the limits for its existence for a certain set of parameters. It is found that the steady-state velocity of the particle is independent of material properties and depends only on the geometry of the system. This means that the particle experiences an effective velocity-dependent friction force, with an effective ''viscosity'' determined only by the geometry. The fluctuations of the motion, however, can depend on the coefficient of restitution e_n. For example, the diffusion coefficient D_x is influenced by e_n, but hardly depends on the roughness of the plane, while for D_y the reverse is true. The range of the inclination angle and the roughness for which a steady state exists also depends on e_n. We discuss how these results can be understood by considering the details of the motion. [S1063-651X(97)09509-3]

PACS number(s): 46.90.+s, 07.05.Tp, 46.30.Pa, 83.70.Fn

I. INTRODUCTION

Granular materials recently have received increasing interest from the physics community [1]. This interest certainly is due to their practical importance, but even more so to the fact that they represent an easily observable system far from thermodynamic equilibrium. Even seemingly simple granular systems can show surprisingly complex behavior. Here we will discuss such a system: a single sphere moving on an inclined plane roughened by gluing spheres to its surface. Figure 1 shows a schematic drawing of the setup.

This system already has been the subject of a number of experimental [2–9] and theoretical [10–13] investigations, but still no complete understanding of the motion has emerged. The reasons for the strong interest in this system lie in the hope of gaining some understanding of the properties of granular flow on inclined surfaces, such as avalanching [14] and segregation in flow in inclined chutes [15], or in rotating drums [16–19], as well as questions about the stability and steady-state properties of flow on inclined surfaces in general.

The advantage of having only a single particle move in an otherwise fixed environment is the nearly perfect control of all important parameters: The slope of the plane can be fixed (and does not vary in time as in an avalanching sand heap or a rotating drum), as well as the roughness of the plane by choosing the radius R of the moving particle and the radius r of the particles on the plane. The particle can be introduced on the plane with a well-defined starting velocity, which is important since this may affect its motion. For many-particle flow in inclined chutes it is still unclear how the flow is affected by the way particles are introduced into the system [20]. The main questions this system poses are the following: Given a size ratio $\Phi = R/r$ of the particles, i.e., the roughness of the plane, and an inclination angle θ, will the particle reach a steady state and if so, is it independent of the initial conditions? How does the friction force exerted on the particle by the bumps on the plane scale with these parameters and how does it depend on material properties such as the coefficient of restitution and the friction coefficient of the particles?

Though we will also discuss briefly the conditions for the existence of a steady state with $\overline{v_x} \neq 0$, here we focus mainly on the properties of the motion *in* the steady state. Experimentally, it was found that the mean velocity is proportional to the driving force, which was interpreted as being due to an effective viscous friction. The mean velocity scales with a power of the size ratio Φ, i.e., for the mean velocity $\overline{v_x}$ of the ball in the steady state $\overline{v_x} \sim \Phi^{\alpha} \sin\theta$, where α seemed to depend slightly on the preparation of the rough plane. Measured values for α were 1.5 [3–5] and 1.05 [8,9] on a plane covered with glass spheres, with different density of the packing and different sizes of the glued beads, and 1.3 on a plane covered with sand [7]. The linear dependence of the velocity on the driving force is surprising on first sight because the velocity loss in each impact should be proportional to the mean velocity, and the number of impacts per unit time should be proportional to the velocity as well. This yields a friction force proportional to $\overline{v_x^2}$ [21] and hence $\overline{v_x} \sim \sqrt{\sin\theta}$. This behavior was actually found in quasi-two-dimensional systems (a ball moving along an inclined line of balls) in both experiment and simulation [2,6,11,12], where it can be explained using a detailed model of the motion

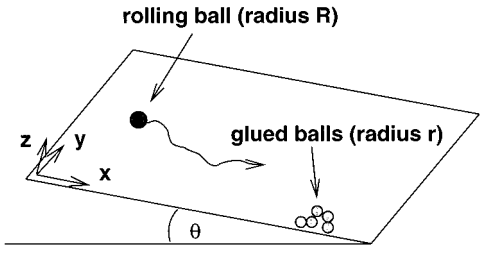

FIG. 1. Schematic drawing of the ball on the plane.

[12]. On the inclined *plane* there seems to be a crossover from linear behavior to a square root for very large and heavy balls and small θ [22]. The reasons for this remain completely unclear so far.

The main difference between the two-dimensional and three-dimensional cases is that in three dimensions (3D) the ball has an additional degree of freedom. It can (and does) move in the direction perpendicular to the inclination of the plane, due to oblique impacts with balls on the plane. This leads to increased dissipation of energy compared to 2D since transverse motion ''drains'' the particle of a part of v_x, as transverse motion is only dissipative. Though certainly v_y can be transferred back to v_x, this only means giving back part of what previously had been lost, so there is only net dissipation due to the additional degree of freedom. But why this increase should lead to *viscous* friction is still unclear.

It thus is necessary to investigate the fluctuations of the motion more closely since they seem to be the key difference between 2D and 3D. Indeed, the argument leading to $\overline{v_x} \sim \sqrt{\sin\theta}$ disregards fluctuations, and as we have shown in previous work [12], these can be neglected in 2D since there the motion is very regular. In 3D, they should be of greater importance. Recent experimental efforts have thus concentrated on the measurement of the dispersion properties of the plane, i.e., on the measurement of diffusion coefficients and their dependence on Φ and θ [8]. These experiments have yielded some surprising results, for example, insensitivity of the longitudinal diffusion coefficient to Φ [8], but the details of the motion that might explain them are inaccessible to experimental observation. Computer simulations can provide this additional information as well as allow variation of material properties far more freely than possible in experiments.

In this paper, we present a fully three-dimensional simulation of this system. Previous simulations were either restricted to two dimensions [6,11,12] or dealt only with questions of static equilibrium of balls on the plane [4]. The outline of the paper is as follows. In Sec. II we will briefly explain the extension of the simulation method we used in 2D to 3D. We will then discuss the results obtained. There, we will first present more global properties of the motion that can be compared with experimental results, as well as the influence of material parameters such as the coefficient of restitution on these properties. To explain some of these results, in the following we concentrate on the details of the motion inaccessible to experiments. As in the two-dimensional case, these reveal the dissipation mechanism active in the steady state and thus explain the insensitivity of some of the global properties of the motion to material properties. Finally, we discuss the consequences this has for the differences and common features of the two- and three-dimensional cases and compare our results with experiments and a previously proposed model of the motion.

II. SIMULATION METHOD AND PREPARATION OF THE PLANE

We simulate the motion by the molecular-dynamics method [23,24], which was introduced to the simulation of granular materials by Cundall and Strack [25]. Particles are treated as ''soft'' (i.e., they can overlap) and interact with some repulsive force only when they overlap. A variety of forces has been used to accomplish this [26]. Here we use the same forces as in our simulation of the two-dimensional case [12], i.e., the force acting between particles i and j is given by

$$\vec{F}_{ij} = F_n \vec{n} + F_s \vec{s}, \tag{1}$$

where

$$F_n = -k_n \xi - \gamma_n \dot{\xi} \tag{2}$$

and

$$F_s = -\min(|\gamma_s v_s|, |\mu F_n|)\,\mathrm{sgn}(v_s). \tag{3}$$

Here ξ denotes the (virtual) overlap of the particles, μ is the Coulomb friction coefficient, and k_n, γ_n, and γ_s are material parameters relating to the stiffness and dissipative properties of the material (for a detailed explanation see [12]). The only difference between the use of these forces in 2D and 3D lies in the definition of the unit vector $\vec{s}$ (the definition of $\vec{n}$ does not change as compared to 2D). In 3D, the direction of the tangential force is given by the *projection* of the velocity vector $\vec{v}$ on the plane perpendicular to $\vec{n}$, since contrary to the two-dimensional case there is a whole plane perpendicular to $\vec{n}$. Thus

$$\vec{n} = \frac{\vec{r}_j - \vec{r}_i}{|\vec{r}_j - \vec{r}_i|}, \tag{4}$$

$$\vec{s} = \frac{\vec{v}_j - \vec{v}_i - [(\vec{v}_j - \vec{v}_i)\cdot\vec{n}]\vec{n} + \vec{n}(R_j\vec{w}_j - R_i\vec{w}_i)}{|\vec{v}_j - \vec{v}_i - [(\vec{v}_j - \vec{v}_i)\cdot\vec{n}]\vec{n} + \vec{n}(R_j\vec{w}_j - R_i w_i)|}. \tag{5}$$

Force (3) can be extended to 3D trivially because it depends only on the instantaneous values of the velocity and the overlap (contrary to some other force laws [27]) and thus is not affected by any memory of changes in the direction of $\vec{s}$.

In all simulations presented here we used the parameters $k_n = 2\times10^5$ N/m, $\gamma_s = 1000$ kg/s, $\mu = 0.13$, $r = 0.5$ mm, and $M = \frac{4}{3}\pi R^3 \rho$ for the mass of the rolling ball with $\rho = 7.8$ g/cm^3. The values of these parameters were chosen to match the steel balls used in [6,5,8] and the size of the glass beads glued onto the inclined plane [8]; the choice of k_n leads to a collision time of the order of 10^{-5} s. For the choice of γ_s, which is mainly a technical parameter, see [12]. The damping γ_n is determined by fixing the normal coefficient of restitution $e_n = -v_n^f / v_n^i$, defined by the ratio of final and initial normal velocities. In this paper, we will show results for $0.4 \leqslant e_n \leqslant 0.8$.

The main problem in the three-dimensional simulation, if it is to be compared with experiments, lies in producing a plane with similar density *and* disorder as in experiments, especially as *disorder* cannot be easily quantified. In the experiments the rough plane was produced by placing a sheet of contact paper on a glass plate and then spreading glass beads onto it slowly moving from one edge of the plane to the other. This gave area fractions of glued beads in a range from 0.68 to 0.74. Algorithms designed to produce random two-dimensional packings, for example, the random sequential adsorption model [4] or more refined versions of it, cannot reach such a high density. To be able to compare our

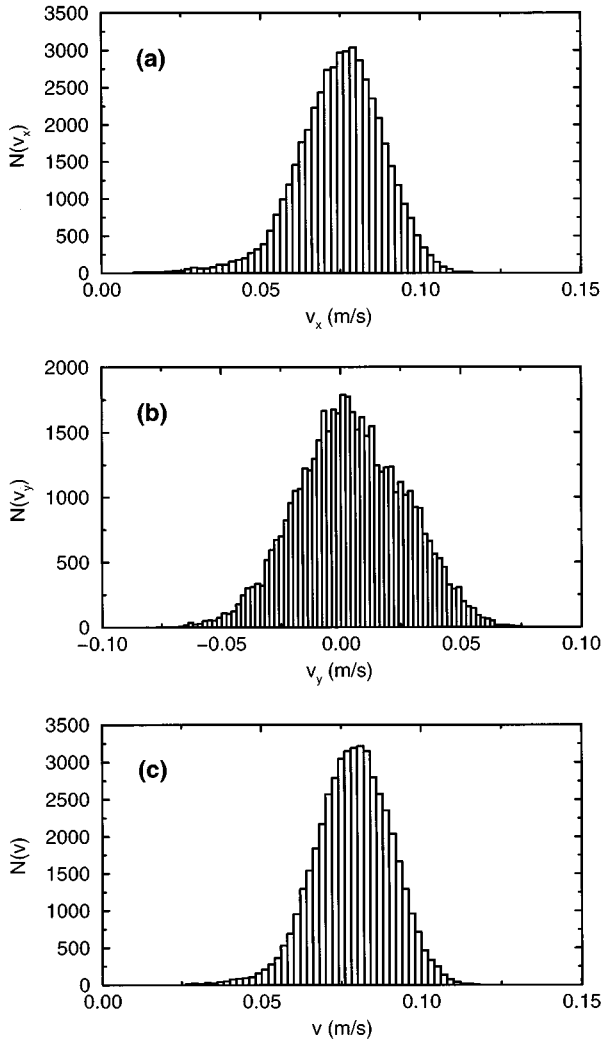

FIG. 2. Histograms of the velocity distributions for $\Phi=5$ and $\theta=0.05$.

results with experiments, we thus used a scanned configuration of the ''real'' plane in the simulations. The section of the plane we used contained 4085 particles and the size was $11.25\times4.35\ \mathrm{cm}^2$. The coordinates of the particles on the boundaries were shifted slightly to create smooth periodic boundaries.

III. SIMULATION RESULTS

A. Average properties

In the simulations presented here, the ball was launched onto the plane with a rather high starting velocity v_x and $v_y=0$. When the ball reached a steady state with $\overline{v_x}\neq0$ for a certain combination of Φ and θ, we averaged over several runs with different starting velocities and starting positions. In each run, the velocity fluctuated somewhat and also the mean velocity varied a bit more from run to run than in 2D. Figure 2 shows typical velocity distributions. The tail towards smaller x velocities corresponds to larger y velocities (see Fig. 3), i.e., to parts of the motion where a lot of x velocity could be transferred to the y direction. Very similar distributions and correlations of v_x and v_y were found in experiments [8]. In Fig. 4(a) we plot the velocity $\overline{v_x}$ for various size ratios Φ as a function of $\sin\theta$ for $e_n=0.8$. Obviously for very large Φ the velocity curves look more like $\sqrt{\sin\theta}$ (though it is hard to decide if the exponent is really 1/2), whereas for smaller Φ the curvature seems to decrease. Unfortunately, the range of inclination angles for which a steady state can be found decreases at a certain point as well and it is very hard to decide over such a small range of inclination angles whether the curves are really linear for small Φ, as seen in the experiments. In Fig. 4(b) the velocities were scaled by a factor $\Phi^{-\alpha}$ with $\alpha=1.5$. This is the same value as that found by Riguidel [3–5]. The sudden rise of the velocity curves corresponds to a similar intermittent motion as observed in two-dimensional simulations [12] and three-dimensional experiments [5], where the ball still maintains a mean constant velocity, but with stronger fluctuations and short accelerating and decelerating phases.

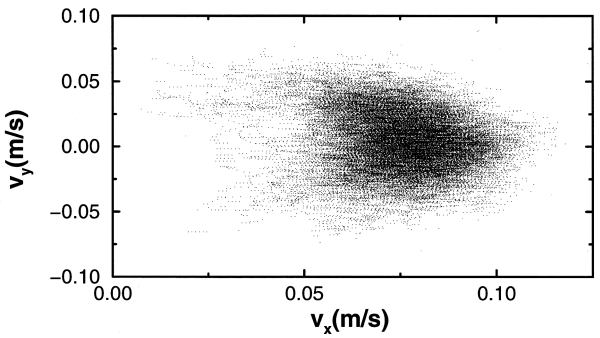

FIG. 3. Correlation of v_x and v_y for the same parameters as in Fig. 2.

Figure 5 shows the phase diagram obtained from these velocity curves. By *phases* here we denote the different kinds of motion. In phase A the particle decelerates and comes to a stop, independently of the velocity with which it

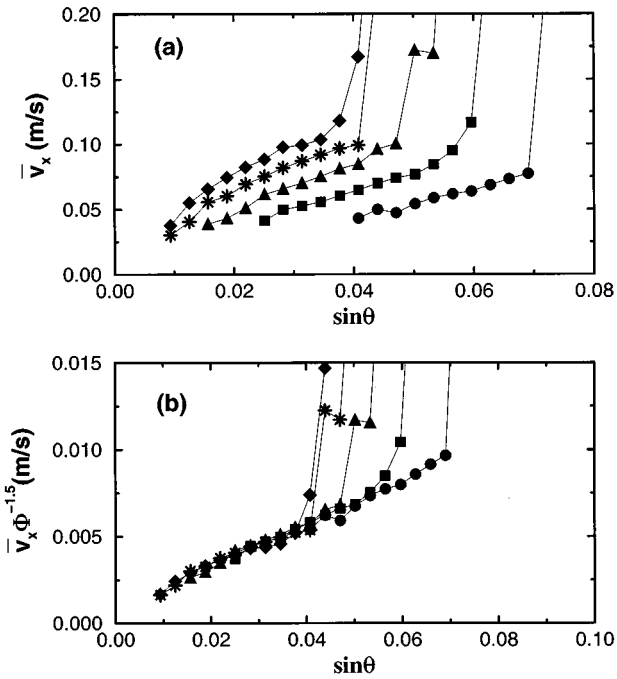

FIG. 4. (a) Mean velocities for $e_n=0.8$ and $\Phi=4$ (circles), $\Phi=5$ (squares), $\Phi=6$ (triangles), $\Phi=7$ (stars), and $\Phi=8$ (diamonds). (b) Scaling of the mean velocities with Φ.

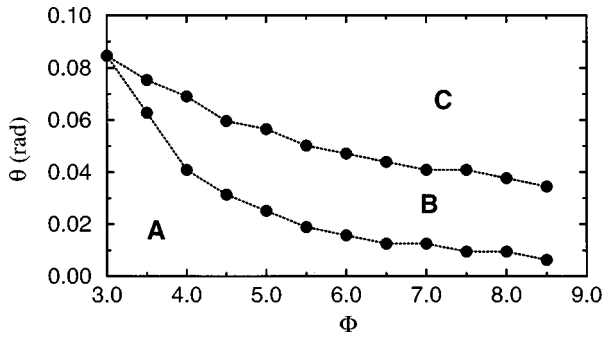

FIG. 5. Phase diagram for $e_n = 0.8$.

was launched on the plane; in phase B it reaches a steady state, independently of the starting velocity; and in phase C it accelerates without reaching a steady state. In region B, sometimes the ball will come to a sudden stop after having previously traveled with constant velocity because it is trapped by a large hole on the plane. This is very clearly distinguishable from stopping in region A, where the ball continuously slows down from the start of the motion. A detailed analysis of this stopping can be found in [28]. Here we are more concerned with motion in region B.

The steady-state region B is much smaller than in experiments and shifted towards smaller θ. In 2D, we have shown that decreasing the coefficient of restitution will hardly affect the steady-state velocity, but instead shift the phase boundary $\theta_{BC}(\Phi)$ towards larger values of θ for a given Φ. One reason that our range of stable θ is too small might be the use of too high a coefficient of restitution. Though $e_n = 0.8$ is appropriate (and even a bit too small) for steel on glass, it is unclear how strong the effect of the combined setup (glass beads on contact paper on glass plate) is. The glued glass beads are not immovably stuck and might shift slightly during impacts. A test performed on the real plane by dropping a steel ball on the horizontal plane resulted in only very little rebound. Still, this does not help in measuring the coefficient of restitution since it cannot be controlled under what angle the ball hit a ball on the plane, so pre- and postcollisional normal velocities are simply not known. We also checked that just like in the two-dimensional case, the coefficient of friction μ does not influence the mean velocity.

To show the effect of e_n, we plot in Fig. 6 the velocity curves for $e_n = 0.4$ and 0.8 together. Here a different picture emerges. The curves already exhibiting definite curvature for

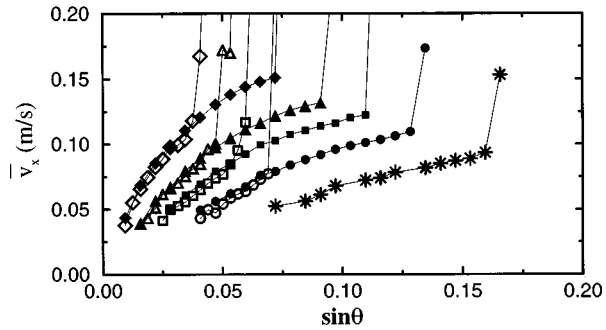

FIG. 6. Mean velocities for $e_n = 0.8$ (open symbols) and $e_n = 0.4$ (closed symbols) and $\Phi = 3$ (stars), $\Phi = 4$ (circles), $\Phi = 5$ (squares), $\Phi = 6$ (triangles), and $\Phi = 8$ (diamonds).

$e_n = 0.8$ hardly deviate from those for $e_n = 0.4$. In the intermediate range of Φ curves that for $e_n = 0.8$ seemed rather linear now prove to be part of lines with definite curvature. For even lower Φ, however, the curves do not fall as nicely on top of each other and there is a small but visible difference in the curvature. For very low Φ (for which we did not even find a steady state for $e_n = 0.8$) the velocity again seems to depend linearly on sin θ. Figure 6 also throws some doubt on the scaling that was found in previous work and in Fig. 4. It is obvious that the velocity curves for $e_n = 0.4$ will not scale with the same exponent as the ones for $e_n = 0.8$. Indeed, only taking into account the upper parts of the curves, where a steady state was found in recent experiments, they will ''scale'' with an exponent $\alpha = 1.05$ [8]. Our simulation results are not very promising as far as the scaling with Φ is concerned.

To us it is not clear yet what conclusions should be drawn from this. There might be a passage from linear behavior to a square root, for which the critical Φ depends on the coefficient of restitution. But the seemingly linear curves might as well just be part of a square root and the curves too short to decide this. It is also not completely clear if there might be a fundamental difference between experiment and simulation. We will return to this point later, in the light of other simulation results. The experimental values look linear, but the range of angles over which they were obtained is so small that they are fitted equally well by a line and a square root.

B. Fluctuations

As stated before, the velocity of the particle fluctuates around the mean velocity depicted in Figs. 4 and 6. These fluctuations should be interesting for the ability of the plane to promote segregation in the transverse direction. In addition, it should be expected that fluctuations affect the phase boundaries (the stronger the fluctuations in the longitudinal direction, the higher the probability that close to θ_{AB} the ball may be trapped and that close to θ_{BC} the ball may achieve a velocity that cannot be braked anymore). In the direction transverse to the main direction of motion, the particle undergoes a diffusive motion [8,29], and in a reference frame moving with $\overline{v_x}$ with the particle, the same is true for the longitudinal direction. Though the corresponding velocity distributions are not perfectly Gaussian, as is obvious from Fig. 2, we define transverse and longitudinal diffusion coefficients by

$$D_x = \lim_{t\to\infty} \langle [x(t) - x(0) - \overline{v_x} t]^2 \rangle / 2t, \tag{6}$$

$$D_y = \lim_{t\to\infty} \langle [y(t) - y(0)]^2 \rangle / 2t. \tag{7}$$

In Fig. 7 the diffusion coefficients obtained in our simulations for various size ratios and $e_n = 0.4$ are shown. They were obtained by performing several long runs (100 s each) with different initial conditions and then cutting these down to pieces of different length, up to 3 s each to perform the ensemble average. Because of the anisotropy in the system introduced by gravity, we expect anisotropy in the diffusion coefficients as well and thus compute them separately. Con-

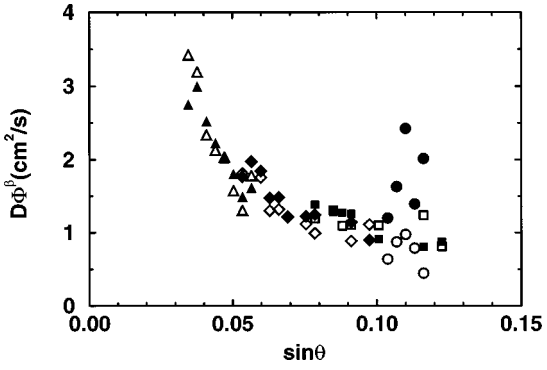

FIG. 7. Diffusion coefficient for $e_n=0.4$ and various size ratios. $\Phi=3$ (circles), $\Phi=4$ (squares), $\Phi=5$ (diamonds), and $\Phi=6$ (triangles). Open symbols, $D_y, \beta=0$; full symbols, $D_x, \beta=1.5$.

trary to [29], where we plotted D_x and D_y as functions of the mean velocity $\overline{v_x}$, here we show them as functions of sin θ. This is the quantity that in any practical application, where segregation might play a role, will be important since the inclination will usually be at some fixed value while the velocity may evolve freely. In Fig. 7, $D_x\Phi^{1.5}$ instead of D_x is plotted since we found that this makes D_x and D_y fall approximately on the same curve.

The diffusion coefficients we find are in good agreement with experimental values [8,29] and are obviously decreasing with increasing angle of inclination. Note that when D_x is scaled by $\Phi^{1.5}$, the values for D_x and D_y are of approximately the same magnitude, i.e., there is a Φ-dependent anisotropy in the diffusion coefficients. A similar anisotropy is found in sedimentation, where, however, the diffusion coefficient corresponding to the mean direction of motion is larger than the one corresponding to the transverse direction [31]. In our case, the reverse is true.

In Fig. 8 the diffusion coefficients are shown for two different values of e_n, this time without any scaling. Though for D_y the data for $e_n=0.8$ fall more or less on the same curve as those for $e_n=0.4$, for D_x they seem to be larger by approximately a factor of 2 for $e_n=0.8$ as compared to $e_n=0.4$. They thus cannot be scaled by the same factor Φ^{β} to make them collapse on the D_y curve. We will return to this later and discuss possible reasons, when we know more about the details of the motion.

C. Details of the motion

In the two-dimensional case, many of the global properties of the motion could be explained by analyzing details of the motion, such as distributions of the points on the surface bumps that were impacted by the moving ball, or correlations between these and the normal and tangential velocities in these impacts [12]. They revealed that the motion in the two-dimensional case, even if the arrangement of balls on the line is disordered, is very regular. This regularity results from the tendency of the ball to collide with the same ball in the line many times, thus losing most of its normal velocity, retaining only tangential velocity with respect to the surface of this particular ball. In the steady state, this leads to quite a well-defined tangential velocity, with which the moving ball rolls onto the next ball on the line. With respect to the new ball the velocity has a normal component. The steady state is

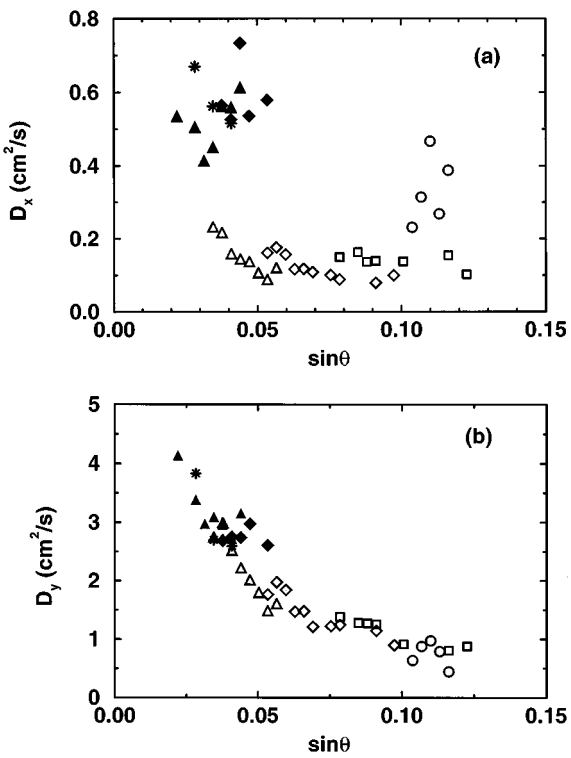

FIG. 8. Dependence of diffusion coefficients on e_n. Full symbols, $e_n=0.8$; open symbols, $e_n=0.4$. For the various Φ values, symbols are the same as in Fig. 7. The stars correspond to $\Phi=5.5$, $e_n=0.8$.

maintained because tangential velocity gained in moving down the plane is converted to normal velocity, which is then dissipated. Because even on a line with disorder the distance throughout which the moving ball can achieve this loss of normal velocity before impacting the next ball is relatively well defined, this leads to strong regularity in the motion, with collisions at approximately the same points on the surface of each ball.

In 3D, one would expect this not to hold any more, since in 3D there are many influences that prevent such strong regularity. When the ball collides with a ball on the plane slightly sideways, it is deflected towards the side. Thus the direction of motion changes at this point. Also the distance traveled over this ball before hitting the next one may be much smaller than the diameter of a ball on the plane. Some of these possibilities are shown on the left-hand side of Fig. 9, assuming that the direction of motion is hardly affected by interaction with the curved surface of the ball. The ball might also roll down the plane without going over the tops of the balls on the plane, moving mainly in the valleys formed by the bumps of the surface. A completely different possibility is that it might be deflected by the first impact with a ball on the plane so strongly that it could jump over to another ball immediately. Considering these possibilities, it has to be kept in mind that the area on the balls on the plane that is accessible to the moving ball is very small and only very slightly curved due to the large values of Φ.

The details of the motion we focus on here are essentially the same as in the two-dimensional case, namely, the times of flight between two impacts with balls on the plane and the exact locations where balls on the plane are hit. Since these

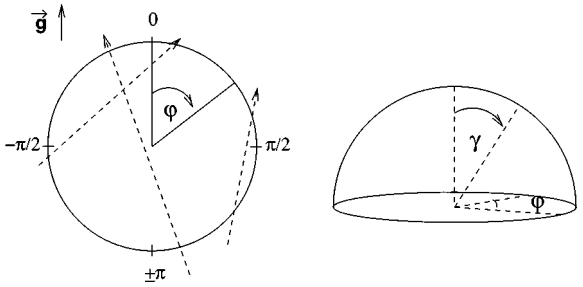

FIG. 9. Definition of the impact angles. Left: view of a ball on the plane from the top and definition of the azimuthal angle φ. The dashed arrows show possible paths the moving ball may take. Right: view of a ball on the plane from the side and definition of γ.

details are extremely hard to access in experiments, computer simulations provide a useful tool to supplement experimental data. These quantities are of interest because the times between collisions give an estimate of the time during which energy can be gained by the particle, while the angles where the impacts take place show how far the detailed topology of the plane is explored by the ball.

Figure 10 shows distributions of times between two successive collisions for two different inclination angles θ and two strongly different coefficients of restitution. The values of θ were chosen such that they lie close to the lower and upper boundaries of the region B, respectively, for the coefficient of restitution in question (see Fig. 6). We separated impacts on the uphill facing side of the balls on the plane ($|\varphi| \geqslant \pi/2$; see Fig. 9) from those on the downhill facing side ($|\varphi| < \pi/2$). As a matter of fact, this is quite an arbitrary way of separating the distributions, as we will see, but we adopt it to enable later comparison with results from the stochastic model from Ref. [10]. The most important difference between collisions at $|\varphi| \geqslant \pi/2$ and $|\varphi| < \pi/2$ is that in a collision at $|\varphi| \geqslant \pi/2$, v_x is transferred to v_z, while for $|\varphi| < \pi/2$, v_z is transferred to v_x. This means that collisions on the uphill facing side of the bumps drive the particle away from the plane, while collisions on the downhill facing side drive it towards the plane. As in 2D, the times between collisions are on average smaller (and some very close to zero) for $|\varphi| < \pi/2$ than for $|\varphi| \geqslant \pi/2$, in contradiction to [10]. When the inclination angle increases, both distributions get broader, but the pronounced decay of the distribution for $|\varphi| < \pi/2$ remains, whereas the peaks of the distribution for $|\varphi| \geqslant \pi/2$ move towards larger times. Multiplying the times between collisions by the mean velocity, we find that the corresponding distances passed between impacts are much smaller than a particle radius.

Obviously, the overall shapes of the distributions depend far stronger on the coefficient of restitution than on the inclination angle. While the total distribution for $e_n = 0.8$ is essentially a decaying function, the distribution for $e_n = 0.4$ rather consists of multiple peaks, getting narrower with smaller times of flight. In addition, the form of the distributions corresponding to $|\varphi| < \pi/2$ and $|\varphi| \geqslant \pi/2$, respectively changes, losing some peaks for $|\varphi| \geqslant \pi/2$ and gaining some for $|\varphi| < \pi/2$. While the shape of the distributions is largely unaffected by θ, they generally extend towards larger times with increasing θ, and for $e_n = 0.8$, a shoulder develops for higher θ.

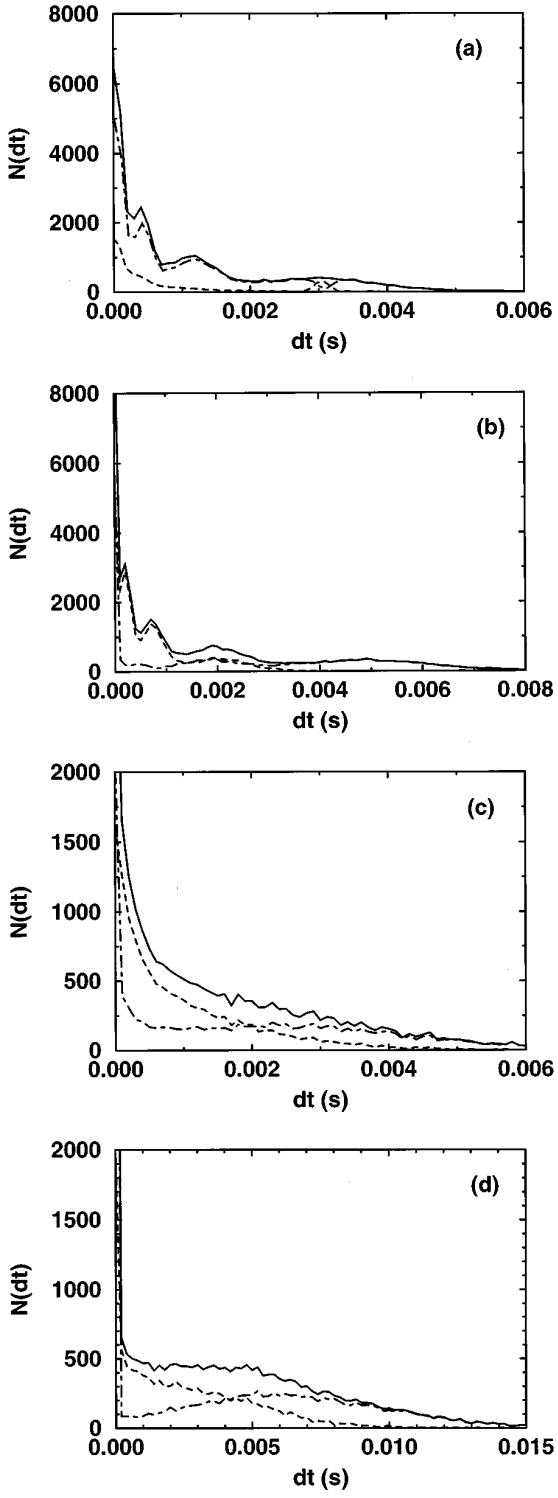

FIG. 10. Histograms of times between collisions for $\Phi = 5$ and (a) $e_n = 0.4$, $\theta = 0.05$, and $\overline{v_x} = 8.2$ cm/s; (b) $e_n = 0.4$, $\theta = 0.08$, and $\overline{v_x} = 10.7$ cm/s; (c) $e_n = 0.8$, $\theta = 0.03$, and $\overline{v_x} = 5.1$ cm/s; and (d) $e_n = 0.8$, $\theta = 0.05$, and $\overline{v_x} = 7.8$ cm/s. Full line, total distribution; dashed line, previous impact at $|\varphi| < \pi/2$; dot-dashed line, previous impact at $|\varphi| \geqslant \pi/2$.

A quantity that has not been measured experimentally yet, and would indeed be very hard to measure, is the distribution of impact angles, i.e., *where* exactly impacts take place on the ball on the plane. The definition of the angles is given in Fig. 9. Figures 11 and 12 show these angle distributions for

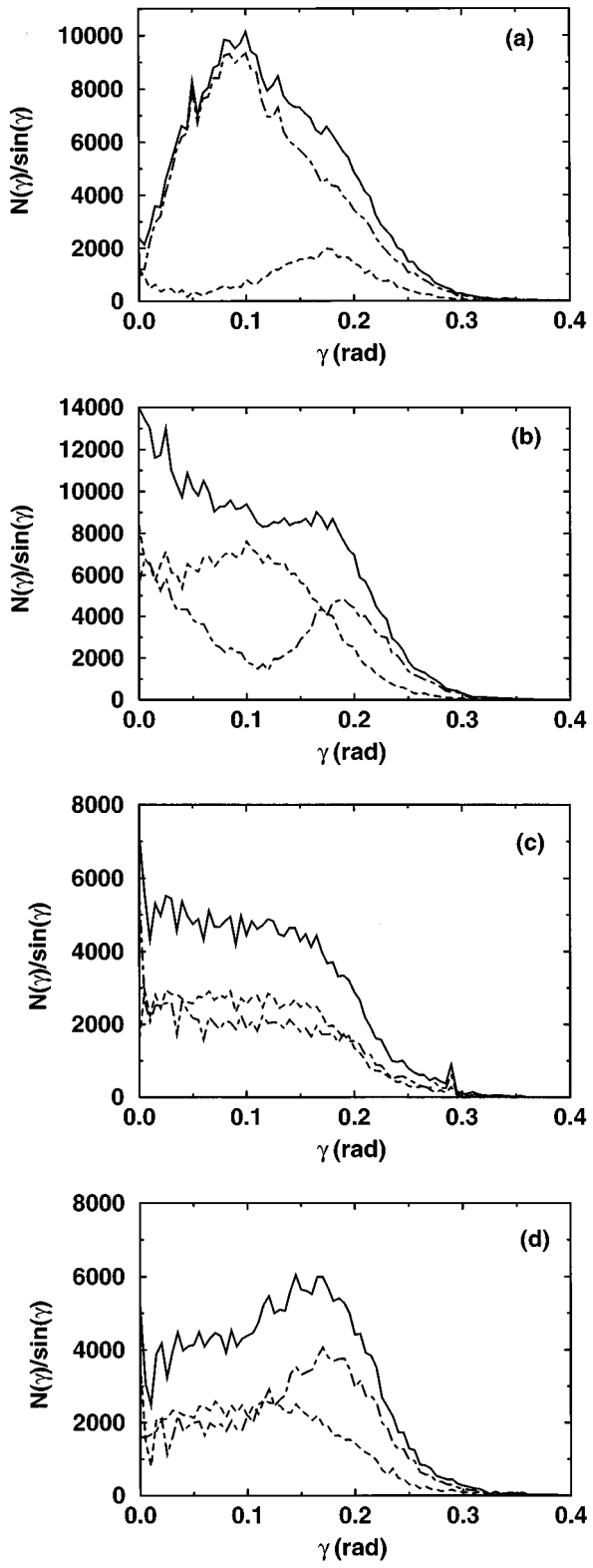

FIG. 11. Histograms of impact angles γ, same parameters as in Fig. 10.

the same cases as the distributions of times of flight in Fig. 10. In the case of γ we plot $N(\gamma)/\sin(\gamma)$ to normalize the distributions by the size of the corresponding volume element.

Unfortunately, even though for $e_n=0.4$ some structure seems to be evident, it is not at all as clear from these distributions as in the two-dimensional case what exactly is happening as the ball moves down the plane. As in the case of the times of flight distributions, for $e_n=0.8$ the shape of the distributions does not change very much with increasing θ, though the one corresponding to $|\varphi|\geqslant\pi/2$ develops a pronounced peak. Figure 11(c) corresponds to a run where the ball, after having moved a distance of 2 m on the plane with constant mean velocity, suddenly stops because it gets trapped by a large hole; hence results the small peak at $\gamma=0.3$, which corresponds to the depth of the hole where the ball got trapped. For $e_n=0.4$, the distributions again change quite significantly in form with changing θ, just like those for the times between collisions. Another point that might be noted is that for $e_n=0.4$ the distribution shows more collisions towards the top of balls on the plane with increasing θ, while for $e_n=0.8$ the number of collisions at the top of balls on the plane decreases with increasing θ. This increase and decrease, respectively, is entirely due to the change in the distribution corresponding to $|\varphi|<\pi/2$.

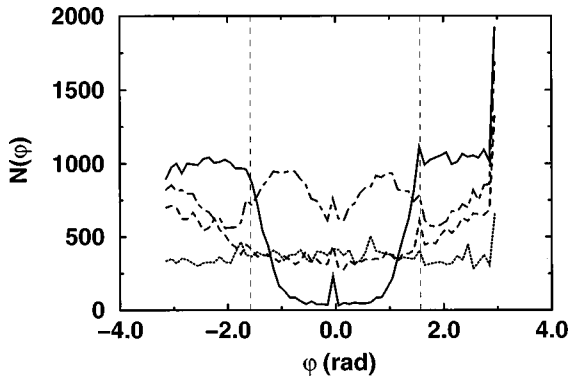

FIG. 12. Histograms of impact angles φ. The vertical dashed lines indicate $\pm\pi/2$. $\Phi=5$, $e_n=0.4$, and $\theta=0.05$ (full line); $\theta=0.08$ (dot-dashed line); $e_n=0.8$ and $\theta=0.03$ (dotted line); $\theta=0.05$ (dashed line).

Though the distributions for times of flight and impact angles γ were already separated according to the side of the ball on which the impact takes place, it is quite instructive to have a more detailed look at the azimuthal angles φ where impacts take place. Figure 12 shows these distributions for the same cases as depicted in Figs. 10 and 11. Again, there are quite strong differences between the different coefficients of restitution. While for $e_n=0.8$ the distribution for smaller θ is uniform, for larger θ it starts to develop a peak on the uphill side, which clearly corresponds to the peak for γ in Fig. 11(d). For $e_n=0.4$, most impacts are on the uphill side of balls on the plane and only very few on the downhill side (with a uniform distribution on the uphill side) for small θ. For larger θ, this uniform distribution forms a peak similar to the one for $e_n=0.8$ and two additional peaks develop symmetrically on the downhill side.

All these details taken separately give a somewhat confusing picture. But adding one more detail that can be extracted from the simulation, the mechanism providing the friction force that maintains the steady-state velocity becomes clear. The quantity that reveals what happens in detail on each ball on the plane is the loss of normal velocity per particle passed, i.e., how the normal velocity *after* the last impact with a certain ball relates to the normal velocity *be-*

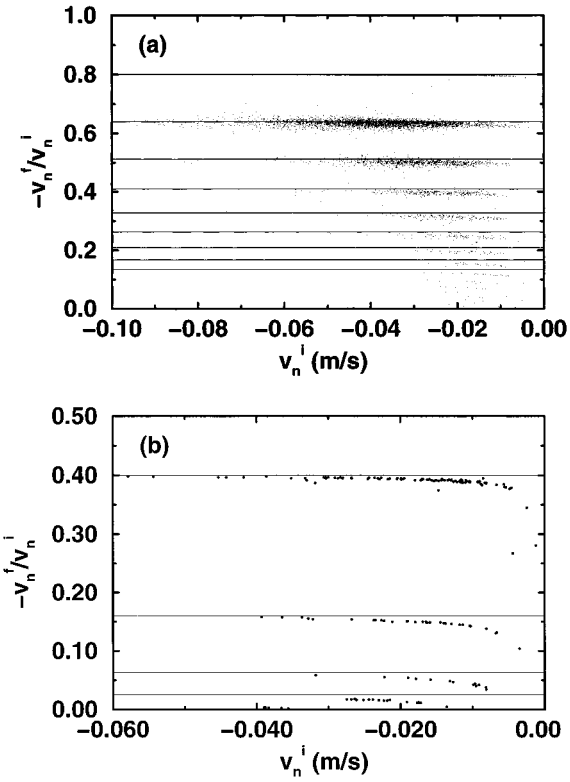

FIG. 13. Relation of normal velocity directly after the last impact with a ball on the plane to normal velocity directly before the first impact with the same ball for $\Phi=5$, $\theta=0.05$, and (a) $e_n=0.8$ and (b) $e_n=0.4$. The lines denote integer powers of the corresponding restitution coefficient.

fore the first impact with the same ball on the plane. Figure 13 shows the relation of these velocities for two different coefficients of restitution at the same angle of inclination of the plane.

Obviously, all points cluster around integer powers of e_n; for $e_n=0.4$ most of the time all normal velocity with respect to the ball passed is lost, i.e., most points concide with the x axis. In both cases, only the points where $v_n^f \neq 0$ are shown. This is the reason for the small number of points in Fig. 13(b), because here, most of the time, all v_n^i can be dissipated on each ball passed. In Fig. 13(b) 98% of the points coincide with the x axis, versus only 7% in Fig. 13(a). Since in the tangential direction nearly no velocity is dissipated, this means that the amount of dissipation on passing a ball is simply determined by the normal velocity in the first impact and the number of collisions with this particular ball (which can be read off from Fig. 13 for each point). In fact, this is very similar to the two-dimensional system [12]; the only difference is the larger variation of the number of collisions per ball in the three-dimensional case. We will discuss the results obtained and their implications for the mean properties of the motion in the following section.

IV. DISCUSSION OF THE RESULTS

A. Discussion of the simulation results

With the help of the last observation in the preceding section, the results shown previously on the distributions of times between collisions, impact angles, etc., can be explained quite easily and the mechanism by which the particle maintains the steady-state velocity becomes clear. Essentially, this mechanism is the same as in the two-dimensional case. Obviously, the ball does not move down the plane by randomly hopping from particle to particle, but rather, when it arrives at a bead, it collides with it several times. Since we are dealing with a single ball, it can roll freely and thus most dissipation comes from the part of the normal component of the velocity lost in collisions and *not* from frictional contacts, where the tangential velocity might play a role.

As Fig. 13 shows, there are usually a number of impacts with each ball on the plane. In this succession of impacts, the velocity of the moving ball aligns with the tangent to the surface of the ball it is passing since it gains velocity in the tangential direction and loses velocity in the normal direction. If this alignment succeeded for the whole surface of the plane, as it would on a perfectly smooth plane, the ball would go on accelerating. However, our plane is too rough to allow this. Whenever this alignment succeeds, the rolling ball will roll onto another ball on the plane from which it rebounds. This collision transfers velocity tangential to the local plane surface to velocity normal to the local plane surface, which can then be dissipated. This mechanism is the same as in the two-dimensional case; the only difference here is that there is a much larger variation in the distances available for the ball to adjust to the surface of a ball it is passing in 3D (see Fig. 9). This larger variation is also obvious from Fig. 13(a): In a very large number of cases, especially close to θ_{BC}, there are only one or two impacts with each ball on the plane because very often a ball on the plane is passed close to the side. Thus, quite often, the adjustment succeeds only imperfectly for high e_n. However, this does not seem to be too important as long as once in a while all v_n is lost. Already in the two-dimensional case, such behavior was observed for high coefficients of restitution. Such ''leftover'' v_n (or rather the larger part of it, some transfers back into v_t) is added to the freshly gained v_n and partially dissipated on the next bump. The main effect of leftover v_n, which tends to destabilize the motion, is the fact that this leads to a first collision with the next bump at smaller γ, which leads to less efficient transfer of v_t to v_n.

Another reason for the larger variation in the number of collisions with the balls passed is the fact that this first impact, besides transferring tangential velocity to normal velocity, may also change the direction of the tangential velocity with respect to the plane. This change should be the main source of the diffusive motion the particle performs in the transverse direction. When the particle rolls, the curvature of the ball surface on which the particle moves is so small that it has only a minor influence on the motion (recall the typical range of γ accessed by the ball as shown in Fig. 11).

Having identified the mechanism by which the steady state is maintained, we will now discuss how this helps us to understand better the details of the motion presented in Sec. III. Let us first take a look at the distributions of γ in Fig. 11. For $e_n=0.4$, dissipation is so strong that already after the first impact balls have lost so much normal velocity that they do not jump very far. The drop of the distribution towards $\gamma=0$ is not an indication that the ball does not pass over the top of the bumps, but is rather due to the fact that it does not manage to jump over the top, but rolls. This is exactly the

same behavior we found in the two-dimensional case at small inclination angles. The decay of the distribution towards larger γ and partly the small peak for impacts on the downhill side corresponds to the distribution of distances between balls on the line. Note that whenever a peak appears in the distributions shown, it is at approximately the same point and has approximately the same form. For $e_n=0.8$, especially close to θ_{AB}, there are so many collisions on each ball that the number of collisions remains high close to $\gamma=0$, while for higher inclination angles, the peak is quite prominent. This is probably due to the fact that the first jump on each ball carries the ball far enough away from the first impact, so the peak does not get smeared out so strongly as for lower inclination angles. This is probably the same reason for the partly emerging second peak for impacts on the uphill side in Fig. 11(b).

The distributions of impact angles φ in Fig. 12 confirm this. Whereas for $e_n=0.4$ at lower angles of inclination nearly all impacts are on the uphill side, we find two new peaks emerging for higher angles of inclination, obviously corresponding to the second peak close to $\gamma=0$ and the third one close to $\gamma=0.1$ in Fig. 11(b), i.e., balls now manage to *jump* over to the downhill side. For $e_n=0.8$, we again find the same characteristics as described for γ, i.e., with increasing θ there seem to be more impacts on the uphill side than on the downhill side. The main reason is that the first impact in most cases takes place on the uphill side, but either this first impact may remain the only one or the following ones will occur in its vicinity. The distributions of the times between collisions (Fig. 10) show these multiple collisions quite clearly for $e_n=0.4$, while for $e_n=0.8$, the distributions for the single collisions are smeared out too much to be distinguished.

All these details help one to understand some of the global properties of the motion discussed in Sec. III A. The fact that the steady-state velocity $\overline{v_x}$, and thus the effective friction force ''felt'' by the particle, hardly depends on the coefficient of restitution can be explained in the same way as in the two-dimensional case. Since the amount of energy dissipated mainly depends on how much tangential velocity is converted into normal velocity in the first collision with each ball on the plane passed, which in turn is determined only by the geometry of the impact, but not by e_n, it is not surprising that the steady-state velocity does not depend on e_n. The same is valid for the lower boundary θ_{AB} of the steady-state region, just like in the two-dimensional case. The ball only gets stuck when it cannot roll out of the deepest valleys any more. The upper boundary θ_{BC}, however, does depend on e_n because e_n determines how many bounces on each ball are necessary to lose a large part of the normal velocity with respect to each ball before the next one on the plane is hit; if this is not possible, the ball accelerates.

Even if the angle of inclination is too large for the particle to reach a steady state and it constantly accelerates, it tries to adjust its velocity to the direction of the surface. When the ball has a considerably large z velocity, the locations (and thus impact angles) of its collisions are uncorrelated: On average it feels dissipation normal to the plane as a whole and acceleration parallel to the plane. It is thus driven towards the plane more and more. At some point of this evolution, the particle starts to feel the structure of the plane; when collisions get very oblique, not all impact angles are possible anymore and impacts on the uphill facing side of particles on the plane are favored. But these impacts transfer velocity tangential to the plane into velocity normal to the plane; the ball is thus driven away from the plane again. While in the steady state the amount of velocity transferred to the normal direction does not suffice to carry the ball over to the next ball on the plane, in region C it may kick the ball up very high, thus allowing it to gain a larger amount of v_x than it lost in this previous impact. In the accelerating regime, the ball is driven towards and away from the plane continuously. This results from a competition of the ball's efforts to align its velocity to the plane surface and violent impacts on the uphill facing side of surface bumps, which drive it away again if it comes too close, i.e., the ratio v_z/v_x gets too small.

Since the explanations we have just given are the same as in the two-dimensional case, the question arises as to whether we can calculate the mean velocity as in the two-dimensional case by treating the ball as completely inelastic and perfectly rough. In the two-dimensional case, the disorder of the plane can simply be incorporated into the calculation by assuming the balls on the plane to be equally spaced, with a spacing corresponding to the mean value of the distribution of distances. Here this does not suffice. In the three-dimensional case, it is also important to estimate the amount by which the ball will be deflected in the transverse direction. When moving at an angle δ with respect to the x direction, the ball suffers the same number of impacts as if it were moving in the x direction since the number of collisions it suffers in crossing a certain length does not change. But it is moving *down* the plane more slowly and thus gains energy more slowly. Obviously, this additional dissipation has a strong influence on the motion, since in 3D the average Φ where the motion of a ball can be stable is significantly larger than in 2D. So far, we have not found a reasonable assumption that would incorporate this scattering in the transverse direction in a simple calculation since unfortunately this amount of scattering changes with increasing plane inclination.

This leads us to a completely different feature in the three-dimensional case, namely, the fluctuations of the motion. In our case these are measured by calculating the diffusion coefficients corresponding to the longitudinal and transverse directions of motion (separately, because the system is highly anisotropic). Again, we can only discuss qualitatively the possible reasons for their θ and Φ dependence. As we have just explained, the very first impact of the moving ball on each ball on the plane with which it interacts seems to be crucial in determining its motion over this single ball. One might thus expect that this is true as well for the direction into which the ball is scattered in this single impact. Though the changes Δv_x and Δv_y in a single impact depend on e_n, this dependence falls out of the quotient $\Delta v_x/\Delta v_y$ that determines the change of direction in this impact. Since the diffusion in the transverse direction is mainly due to such changes in the direction of the motion, this is to be the reason for the insensitivity of D_y to e_n. D_x should be composed of two components: one resulting from scattering in the y direction, and thus related to D_y, and another one resulting from variations in the number of collisons per ball (i.e.,

variations in the loss of normal velocity per ball). These variations get stronger with increasing e_n and exist in the two-dimensional case as well, which could be the reason for the dependence of D_x on e_n.

Far more puzzling is the dependence of the diffusion coefficients on Φ, namely, that D_x is independent of Φ, while $D_y \approx \Phi^{\beta} D_x$, with an exponent β that seems to depend on the coefficient of restitution. So far, we have not found an explanation for the observation that the transverse coefficient of diffusion depends on the Φ, while the longitudinal one does not.

The slight falling tendency for the diffusion coefficients with increasing θ is easier to explain. Since we suppose that the diffusion is largely due to the scattering of the ball in the first impact with each ball on the plane it interacts with, it should depend on the distribution of these impacts. The more head-on the impact, the smaller the scattering to the transverse direction, the more oblique, and the stronger this scattering. Figure 11 shows that with increasing θ, these impacts became less oblique, so scattering should be reduced and thus diffusion should be reduced.

B. Comparison with experimental results and a stochastic model of the motion

As already mentioned briefly in Sec. II, the agreement of simulations with experiments is not perfect. The mean velocities we find are slightly too high: θ_{AB} is lower than the values found in experiments; for e_n values corresponding to steel on glass collisions θ_{BC} is smaller than in experiments as well. The fluctuations (diffusion coefficients, etc.) are on average smaller in our simulations than in experiments, which might be a reason why the mean quantities are larger, since in granular materials dissipation usually increases with increased fluctuations (e.g., granular temperature) [30]. However, our simulation is not a perfect duplicate of the experimental setup. Some points that differ are the following. The particles in the simulation are perfectly rigidly fixed to the plane. They are perfectly spherical and monodisperse. These conditions are not given in that rigor in the experimental situation and it is not clear how important this might be especially for angles of inclination where a large part of the motion consists of rolling. The adhesion of balls on self-adhesive tape is probably not as perfect as one would wish for, which could lead to strongly reduced and maybe even angle-dependent coefficients of restitution. Even nearly perfect adhesion of a bead to a plate can reduce the coefficient of restitution by approximately 10% [32].

Also in the details of the motion, namely, in the times between collisions, there is some disagreement between experimental results [33] and our simulation results. This discrepancy between experiment and simulation may be explained by the lower resolution of the experimental measurement techniques. The times between collisions extracted from noise measurements in experiments are (translated into distances) of the order of the radii of the balls on the plane, i.e., much larger than in the simulations. As mentioned above, we find best agreement of our simulation data with experimental results for lower coefficients of restitution, such as $e_n = 0.4$. If e_n is that low in the experiments, already the second and third collisions on the same ball take place with strongly reduced normal velocity and thus with far less noise than the first one. In addition, the resolution of the noise measurements is far smaller than in our simulations, so in the experiments times between collisions as small as ours may not be resolved anymore. But if only the first collision with each ball on the plane is loud enough to be recorded, this means that not the time between single collisions but rather the time spent interacting with each ball on the plane is measured. This time can also be extracted from our simulations and is shown for two different e_n in Fig. 14. We plotted $\overline{v_x} dt/r$ on the x axis to give an idea about the corresponding distances. These distributions agree nicely with the times between collisions measured in experiments.

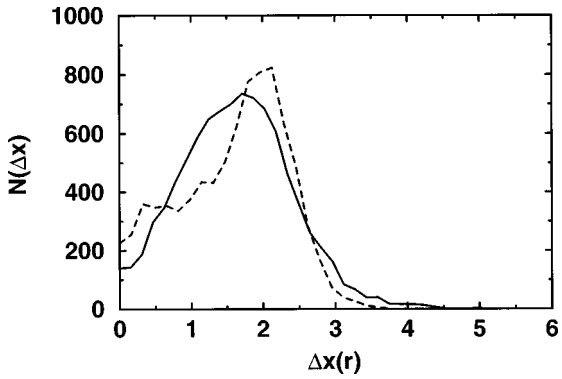

FIG. 14. Total time spent interacting with the same ball on the plane, translated into distances in units of particle radius of the small particles. Both curves are for $\Phi = 5$ and $\theta = 0.05$; the full line for $e_n = 0.8$ and the dashed line is for $e_n = 0.4$.

In the stochastic model of Ref. [10], a clear double-peak structure is found, which disagrees with both simulation and experiment. The times between collisions are of the same order of magnitude as in our model for $|\varphi| \geq \pi/2$ for small θ, while for $|\varphi| < \pi/2$ they are of the same order of magnitude as in experiments. The experimental data show no evidence of a double peak. In the stochastic model, these peaks are clearly separated from each other and the peak at smaller times corresponds to $|\varphi| \geq \pi/2$, i.e., to times after collisions at the uphill side of balls on the plane. Even if we would interpret the decaying distribution and the very broad peak in Figs. 10(c) and 10(d) as two peaks, they disagree with the stochastic model since then on average smaller times between collisions would correspond to the downhill side and not the uphill side.

With the results of Sec. III B, this discrepancy can easily be explained. It arises from the way these times are determined in the stochastic model. There, the time of flight depends on whether the previous impact occurred at the uphill or downhill side of a ball on the plane. If it was on the uphill side, the time of flight is assumed to be $2v_z/g$, disregarding the details of the plane surface; if it was on the downhill side, it is assumed that the time of flight is $2r/v_x$. The next impact angle is chosen at random, though from a distribution that reflects the angles actually accessible to the particle due to the obliqueness of the impact.

By contrast, in the simulation it depends not on the exact location of an impact whether the time until the next one is determined by v_x or v_z, but rather on whether the ball is rolling or jumping. If it is rolling, the time until the next

collision is mainly determined by v_t and the distance between the point of onset of rolling and the next ball on the plane. Though the probability of the ball already rolling is higher towards the downhill than the uphill side, no distinction can be made *a priori*. The typical distance moved by a rolling ball before colliding with the next one is usually (especially for higher e_n) much smaller than r, which gives a much smaller time between collisions than the estimate in the stochastic model, where this distance is always $2r$. If the ball is jumping, the time of flight will be determined by v_z or rather by a combination of v_x, v_z and the exact location on a surface bump where the last impact took place. The random choice of impact angles in the stochastic model, even if it takes place under certain geometrical restrictions, is another important difference. In the simulations, we found that in the steady state, if the ball is jumping, successive impacts are highly correlated since the ball is moving in a preferred direction and there are a few impacts on the same ball on the plane. Especially on the uphill side, the ball may be prematurely stopped (compared to the time of flight calculated by disregarding the details of the surface). In the stochastic model, this is taken into account only in calculating the possible impact angles, but not in the calculation of the time of flight. Therefore, the stochastic model on average overestimates the time of flight.

Besides these differences in the details of the motion, there is also a quite significant discrepancy between some global experimental and simulation results and the stochastic model. In the stochastic model, a linear dependence of $\overline{v_x}$ on $\sin\theta$ is found for $6 \leqslant \Phi \leqslant 10$ at angles of inclination $0.1 \lesssim \sin\theta \lesssim 0.3$ and the whole steady-state region extends over a range $0.02 \lesssim \sin\theta \lesssim 0.45$ for these Φ. These angles of inclination are far too high compared to the range found for the steady state in experiments and simulations. The reason probably is that the randomness introduced in the stochastic model leads to much higher dissipation than experienced by the particle in experiments or simulations. In the simulations we find as well that the more random the particle motion gets (like for high e_n as compared to low e_n), the higher dissipation gets. In the steady state, it seems to be more advantageous for the particle to keep as closely to the plane as possible, i.e., to dissipate all the normal velocity gained in moving from one particle to the next as soon as possible, and then move parallel to the surface until the next abrupt change in the surface direction takes place. However, especially when the motion starts to get more irregular, the stochastic model should be appropriate for describing the motion, but still gives a steady state.

The reason for the existence of a steady state for very large θ results from the absence of rotation in the stochastic model. If the particle cannot rotate, but experiences friction, the angle region for which a steady state exists shifts towards significantly larger θ, compared to a rotating particle. In molecular-dynamics simulations of the two-dimensional case, where particle rotation was excluded, we found a steady-state region for $0.2 \lesssim \sin\theta \lesssim 0.4$ for $\Phi = 2.25$ and a friction coefficient $\mu = 0.13$ [34] (the same μ as used in the stochastic model). Since there is friction present in the stochastic model, but the particle cannot rotate, friction is an additional source of dissipation that obviously extends region B to significantly higher θ.

V. SUMMARY

We have presented molecular-dynamics simulations of a single sphere moving on an inclined plane made rough by glueing similar spheres to it. We have shown that the origin of the friction force experienced by the moving sphere in a certain range of inclination angles is essentially the same as in the two-dimensional case discussed in [12]. In the steady state, the moving ball tries to adjust its velocity to each particle on the plane it passes, i.e., it strives to move parallel to the surface. Adjustment of the velocity occurs in a series of small bounces on each ball that is passed, since in each collision velocity normal to the surface is lost. If this adjustment could be achieved permanently, as it would for a ball dropped on a perfectly smooth (though maybe microscopically rough) plane, the ball would never reach a steady state. However, since the direction of the plane surface (i.e., the tangent to the plane) changes abruptly every time the moving sphere passes from one surface asperity to the next, this adjustment can never succeed completely. In this first collision with each ball on the plane part of the previously tangential velocity is transferred to normal velocity due to the change in the direction of the surface. This new normal velocity is subsequently dissipated in the same way.

The coefficient of restitution mainly determines how many collisions with each ball on the plane are necessary to dissipate all or a large amount of this velocity. The main importance of the roughness of the plane is the continuous conversion of energy gained (in moving parallel to the surface) to energy that can be dissipated. This is achieved by transferring velocity from the tangential direction to the normal direction. The plane thus prevents the particle from ''collapsing'' on the plane permanently. We found that a steady state can only be reached if this ''collapse'' or at least a substantial reduction of v_n is achieved on most balls on the plane that are passed. If it can be achieved, it is unimportant in how many collisions this happened; hence results the insensitivity of $\overline{v_x}$ to e_n. This means that in the steady state, the friction force exerted on the particle by the rough plane is unaffected by the velocity loss in a single collision and only determined by the geometrical roughness of the surface.

With the mechanism that maintains the steady-state velocity we could also explain the details of the motion such as distributions of impact angles and distributions of times between collisions. The source for differences between the two-dimensional and three-dimensional cases has become clear. The diffusion coefficients in the transverse and longitudinal directions were found to collapse on a decreasing function of $\sin\theta$ if D_x was scaled by Φ^{β}. The exponent β slightly depended on e_n since D_x did and for $e_n = 0.4$, $\beta \approx 1.5$ was found. By contrast, D_y hardly seemed to be affected by either Φ or e_n. A qualitative explanation could be given for some of these properties with the help of the details of the motion.

Our simulation results have clarified many points in the motion of a single particle on a rough inclined plane, though some details are still unclear and an analytical approach is, contrary to the two-dimensional case, still lacking. However, the main reason for this lack is the fact that the disorder of our plane is not as well defined as in the two-dimensional case and cannot be incorporated in a similar approximation

as easily as in the two-dimensional case. Still, our simulations have revealed one important property of the motion of the ball that might be of relevance also in more complicated flows, namely, the independence of the mean properties in the steady state of e_n. Though in more complicated flows the fluctuations are more important for the overall properties than in the case of the single particle, we expect that some effects of this independence will be visible in many-particle flows as well. We expect this to be especially relevant to flow in inclined chutes, since there, like in the single-particle case, the particle is driven to interact with the dissipative boundary by a constant force, unlike in flow in a vertical pipe, where contact with the boundaries mainly comes about by the fluctuations in the motion. Work along these lines is in progress.

ACKNOWLEDGMENTS

We wish to thank D. Bideau, L. Brendel, C. Henrique, I. Ippolito, and L. Samson for very valuable discussions. This work was supported in part by the Groupement de Recherche CNRS ''Physique des Milieux Hétérogènes Complexes'' and by the HCM European Network ''Cooperative Structures in Complex Media.''

[1] H. M. Jaeger and S. E. Nagel, Science **255**, 1523 (1992); H. M. Jaeger, S. E. Nagel, and R. P. Behringer, Rev. Mod. Phys. **68**, 1259 (1996).

[2] C. D. Jan, H. W. Shen, C. H. Ling, and C. I. Chen, in *Proceedings of the 9th Conference on Engineering Mechanics, College Station, Texas*, edited by L. D. Lutes and J. M. Niedzwecki (American Society of Civil Engineers, New York, 1992), p. 768.

[3] F.-X. Riguidel, R. Jullien, G. H. Ristow, A. Hansen, and D. Bideau, J. Phys. (France) I **4**, 261 (1994).

[4] F.-X. Riguidel, A. Hansen, and D. Bideau, Europhys. Lett. **28**, 13 (1994).

[5] F.-X. Riguidel, Ph.D. thesis, Université de Rennes I, 1994 (unpublished).

[6] G. H. Ristow, F.-X. Riguidel, and D. Bideau, J. Phys. (France) I **4**, 1161 (1994).

[7] A. Aguirre, I. Ippolito, A. Calvo, C. Henrique, and D. Bideau, Powder Technol. (to be published).

[8] L. Samson, I. Ippolito, G. G. Batrouni, and J. Lemaître (unpublished).

[9] D. Bideau, I. Ippolito, L. Samson, G. G. Batrouni, S. Dippel, A. Aguirre, A. Calvo, and C. Henrique, in *Proceedings of HLRZ Workshop on Traffic and Granular Flow*, edited by D. E. Wolf, M. Schreckenberg, and A. Bachem (World Scientific, Singapore, 1996).

[10] G. G. Batrouni, S. Dippel, and L. Samson, Phys. Rev. E **53**, 6496 (1996).

[11] S. Dippel, L. Samson, and G. G. Batrouni, in *Proceedings of HLRZ Workshop on Traffic and Granular Flow* (Ref. [9]), pp. 353–357.

[12] S. Dippel, G. G. Batrouni, and D. E. Wolf, Phys. Rev. E **54**, 6845 (1996).

[13] C. Ancey, P. Evesque, and P. Coussot, J. Phys. (France) I **6**, 725 (1996).

[14] M. Caponeri, S. Douady, S. Fauve, and C. Laroche, in *Mobile Particulate Systems*, edited by E. Guazzelli and L. Oger (Kluwer, Dordrecht, 1995).

[15] S. B. Savage, in *Disorder and Granular Media*, edited by D. Bideau and A. Hansen (Elsevier, Amsterdam, 1993).

[16] F. Cantelaube and D. Bideau, Europhys. Lett. **30**, 133 (1995).

[17] E. Clément, J. Rajchenbach, and J. Duran, Europhys. Lett. **30**, 7 (1995).

[18] O. Zik, D. Levine, S. G. Lipson, S. Strikman, and J. Stavans, Phys. Rev. Lett. **73**, 644 (1994); K. M. Hill, J. Kakalios, Phys. Rev. E **49**, R3610 (1994).

[19] G. Baumann, I. M. Jánosi, and D. E. Wolf, Phys. Rev. E **51**, 1879 (1995).

[20] P. C. Johnson, P. Nott, and R. Jackson, J. Fluid Mech. **210**, 501 (1990).

[21] R. A. Bagnold, Proc. R. Soc. London, Ser. A **225**, 49 (1954).

[22] L. Samson (private communication).

[23] M. P. Allen and D. J. Tildesley, *Computer Simulation of Liquids* (Clarendon, Oxford, 1987).

[24] D. E. Wolf, in *Computational Physics*, edited by K. H. Hoffmann and M. Schreiber (Springer, Berlin, 1996).

[25] P. A. Cundall and O. D. L. Strack, Geotechnique **29**, 47 (1979).

[26] J. Schäfer, S. Dippel, and D. E. Wolf, J. Phys. (France) I **6**, 5 (1996).

[27] O. R. Walton, Mech. Mater. **16**, 239 (1993).

[28] C. Henrique, M. A. Aguirre, S. Dippel, A. Calvo, I. Ippolito, G. G. Batrouni, and D. Bideau (unpublished).

[29] L. Samson, I. Ippolito, S. Dippel, and G. G. Batrouni, in *Powders & Grains 97*, edited by R. P. Behringer and J. T. Jenkins (Balkema, Rotterdam, 1997).

[30] J. Schäfer, Ph.D. thesis, Universität Duisburg, 1996 (unpublished).

[31] W. Kalthoff, S. Schwarzer, G. Ristow, and H. Herrmann, Int. J. Mod. Phys. C **7**, 543 (1996).

[32] A. Lorenz, C. Tuozzolo, and M. Y. Louge, Exp. Mech. (to be published).

[33] C. Henrique, M. A. Aguirre, A. Calvo, I. Ippolito, and D. Bideau, Powder Technol. (to be published).

[34] S. Dippel, G. G. Batrouni, and D. E. Wolf, in *Proceedings of HLRZ Workshop on Friction, Arching, Contact Dynamics*, edited by D. E. Wolf and P. Grassberger (World Scientific, Singapore, 1997).